

- Pace, C. N., & Creighton, T. E. (1986) *J. Mol. Biol.* 188, 477-486.
- Pace, C. N., & Grimsley, G. R. (1988) *Biochemistry* 27, 3242-3246.
- Phillips, S. (1980) *J. Mol. Biol.* 142, 531.
- Ramachandran, G. N., & Sashisekharan, V. (1968) *Adv. Protein Chem.* 23, 283-437.
- Ramakrishnan, C., & Ramachandran, G. N. (1965) *Biophys. J.* 5, 909-933.
- Ravichandran, V., & Subramanian, E. (1981) *Int. J. Pept. Protein Res.* 18, 121-126.
- Sato, S., & Egami, F. (1957) *J. Biochem.* 44, 753-757.
- Schimada, I., & Inagaki, F., (1990) *Biochemistry* 29, 757-764.
- Sevcik, J., Dodson, E. J., & Dodson, G. G. (1991) *Acta Crystallogr. B* 47, 240-253.
- Shirley, B. A., Stanssens, P., Steyaert, J., & Pace, C. N. (1989) *J. Biol. Chem.* 264, 11621-11625.
- Steyaert, J., Hallenga, K., Wyns, L., & Stanssens, P. (1990) *Biochemistry* 29, 9064-9072.
- Steyaert, J., Opsomer, C., Wyns, L., & Stanssens, P. (1991) *Biochemistry* 30, 494-499.
- Sugio, S., Amisaki, T., Ohishi, H., & Tomita, K.-I. (1988) *J. Biochem.* 103, 354-366.
- Takahashi, K. (1971) *J. Biochem.* 70, 945-960.
- Takahashi, K. (1985) *J. Biochem.* 98, 815-817.
- Takahashi, K., & Moore, S. (1982) *The Enzymes* 15, 435-468.
- Walz, F. G., Jr., & Hooverman, L. (1973) *Biochemistry* 15, 2837-2842.
- Walz, F. G., Jr. & Kitareewan, S. (1990) *J. Biol. Chem.* 265, 7127-7137.
- Walz, F. G., Jr., Osterman, H. L., & Libertin, C. (1979) *Arch. Biochem. Biophys.* 195, 95-102.

## Uniform $^{15}\text{N}$ Labeling of a Fungal Peptide: The Structure and Dynamics of an Alamethicin by $^{15}\text{N}$ and $^1\text{H}$ NMR Spectroscopy<sup>†</sup>

Adelinda A. Yee and Joe D. J. O'Neil\*

Department of Chemistry, University of Manitoba, Winnipeg, Manitoba R3T 2N2, Canada

Received July 15, 1991; Revised Manuscript Received December 23, 1991

**ABSTRACT:** An alamethicin, secreted by the fungus *Trichoderma viride* and containing a glutamine at position 18 instead of the usual glutamic acid, has been uniformly labeled with  $^{15}\text{N}$  and purified by HPLC. The extent of  $^{15}\text{N}$  incorporation at individual backbone and side-chain sites was found to vary from 85% to 92%, as measured by spin-echo difference spectroscopy. The proton NMR spectrum of the peptide dissolved in methanol was assigned using correlation spectroscopies and nuclear Overhauser enhancements (NOE) measured in the rotating frame. The  $^{15}\text{N}$  resonances were assigned by the 2D  $^1\text{H}$ - $^{15}\text{N}$  correlation via heteronuclear multiple-quantum coherence experiment. NOEs and  $^3J_{\text{NH}^{\text{C}}\text{H}}$  coupling constants strongly suggest that, in methanol, from Aib-3 to Gly-11, the peptide adopts a predominantly helical conformation, in agreement with previous  $^1\text{H}$  NMR studies [Esposito, G., Carver, J. A., Boyd, J., & Campbell, I. D. (1987) *Biochemistry* 26, 1043-1050; Banerjee, U., Tsui, F.-P., Balasubramanian, T. N., Marshall, G. R., & Chan, S. I. (1983) *J. Mol. Biol.* 165, 757-775]. The conformation of the carboxyl terminus (12-20) is less well determined, partly because the amino acid composition reduces the number of NOEs and coupling constants which can be determined by  $^1\text{H}$  NMR spectroscopy. The  $^3J_{\text{NH}^{\text{C}}\text{H}}$  in the C-terminus suggest the possibility of conformational averaging at Leu-12, Val-15, and Gln-19, an interpretation which is supported by a recent molecular dynamics simulation of the peptide [Fraternali, F. (1990) *Biopolymers* 30, 1083-1099]. The dynamics at each side-chain and backbone nitrogen were measured by the heteronuclear  $^{15}\text{N}\{^1\text{H}\}$  NOE, but these measurements could not confirm a model in which the carboxyl terminus experiences greater conformational freedom than the amino terminus.

**A**lamethicins are a mixture of hydrophobic peptides secreted by the soil fungus *Trichoderma viride* (Meyer & Reusser, 1967). The peptides are assembled enzymatically by non-ribosomal processes (Reusser, 1967; Rindfleisch & Kleinkauf, 1976), are rich in the amino acid  $\alpha$ -aminoisobutyric acid (Aib, B),<sup>1</sup> and usually contain an amino alcohol such as phenylalaninol (O) (Balasubramanian et al., 1981). The so-called peptaibophols are known for their antibacterial activity (Balasubramanian et al., 1981; Jen et al., 1987) and their ability to uncouple oxidative phosphorylation in mitochondria (Mathew et al., 1981). In black lipid bilayers, they induce a conductance which increases exponentially with applied voltage (Eisenberg et al., 1973; Latore et al., 1981), a behavior also

exhibited by the peptides melittin (Tosteson & Tosteson, 1982), gramicidin (Anderson, 1984), and pardaxin (Zagorski et al., 1991). On this basis, these peptides have been used as

<sup>1</sup> Abbreviations: Aib,  $\alpha$ -aminoisobutyric acid; ATCC, American type culture collection; B,  $\alpha$ -aminoisobutyric acid; cw, continuous wave; DQF-COSY, two-dimensional double-quantum filtered correlation spectroscopy; DSS, disodium 2,2-dimethyl-2-silapentane-5-sulfonate;  $\gamma$ , magnetogyric ratio;  $\text{H}_\text{E}$ , syn substituent of a primary amide;  $\text{H}_\text{Z}$ , anti substituent of a primary amide; HMQC, two-dimensional heteronuclear multiple-quantum correlated spectroscopy; HPLC, high-performance liquid chromatography;  $J$ , scalar coupling constant; NMR, nuclear magnetic resonance; NOE, nuclear Overhauser effect; NOESY, two-dimensional nuclear Overhauser enhancement spectroscopy; O, phenylalaninol; ROESY, rotating frame nuclear Overhauser spectroscopy; TOCSY, total correlation spectroscopy; TPPI, time-proportional phase incrementation;  $\tau_\text{c}$ , rotational correlation time; Pho, phenylalaninol.

<sup>†</sup>Supported by the Natural Sciences and Engineering Research Council of Canada and the University of Manitoba.

models for understanding the voltage-gated ion channels found in the nerves and muscles of higher organisms (Hall et al., 1984).

Little is known about the molecular structure of the alamethicin pore although numerous models have been proposed. The structure of an alamethicin monomer crystallized from acetonitrile/methanol solution (10:1) was determined by X-ray diffraction by Fox and Richards (1982). Refinement of the structure to 1.5 Å showed that acetyl-B-P-B-A-B-A-Q-B-V-B-G-L-B-P-V-B-B-E-Q-O (Gisin et al., 1981) is predominantly  $\alpha$ -helical. However, the carbonyls of Aib-10 and Gly-11 form intermolecular hydrogen bonds to solvent, and the Pro-14 imino ring is accommodated by bending the helix axis away from the ring and switching to a  $3_{10}$ -helical hydrogen-bonding pattern (4  $\rightarrow$  1). Another 4  $\rightarrow$  1 hydrogen bond occurs at the C-terminus of the helix. The strong tendency of Aib-containing peptides to adopt helical conformations has been observed in the crystal structures of more than 60 peptides with various sequences and lengths (Karle & Balaram, 1990; Marshall et al., 1990). This has led to the suggestion that Aib-containing peptides form stereochemically rigid helices which might be of value in protein design (Karle & Balaram, 1990).

There is less agreement on the conformation adopted by alamethicin in solution. A 500-MHz  $^1\text{H}$  NMR study of the peptide dissolved in methanol (Esposito et al., 1987) suggested that the conformation is largely similar to that determined by X-ray diffraction (Fox & Richards, 1982). The only deviation from regular helical structure was an extended conformation for the C-terminal dipeptide. However, these results contrast with an earlier NMR study which proposed a partly helical, partly extended, dimeric structure for the protein in methanol (Banerjee et al., 1983; Banerjee & Chan, 1983). Restrained and unrestrained molecular dynamics simulations suggest that the N-terminus (1–9) behaves like a rigid helical rod but that the structure of the C-terminus (12–20) is ill-defined; the two regions are joined by a hinge (10–11) which undergoes large-amplitude motion in the simulations (Fraternali, 1990).

Because of its unusual amino acid composition, some difficulties are encountered in alamethicin structure determination by proton NMR spectroscopy. The eight  $\alpha$ -aminoisobutyric acid residues lack  $\text{C}^\alpha\text{H}$  resonances; this means that neither homonuclear  $^3J_{\text{NH}^\alpha\text{C}^\alpha\text{H}}$  coupling constants (to determine the dihedral angle  $\phi$ ) nor intra- and interresidue NOESY cross peaks to  $\text{C}^\alpha\text{H}$  are available to determine the conformation of the peptide at these residues. Severe overlap of the methyl resonances makes their assignment difficult and reduces further the number of structural constraints which can be determined by  $^1\text{H}$  NMR. Heteronuclear NMR has the potential for significantly increasing the number of measured constraints and thereby improving the precision with which a solution structure can be determined. For residues which lack  $\text{C}^\alpha\text{H}$  resonances, the  $^3J_{\text{NH}^{13}\text{C}^\beta}$  and  $^3J_{\text{NH}^{13}\text{C}^\alpha}$  heteronuclear coupling constants could be used to obtain information about the angle  $\phi$  (Bystrov et al., 1977; Bax et al., 1988). Another approach is to use  $^{15}\text{N}$  NMR to determine constraints which cannot be measured using  $^1\text{H}$  or  $^{13}\text{C}$ . For example, the long-range heteronuclear coupling between a backbone  $^{15}\text{N}$  and the preceding  $\text{C}^\alpha\text{H}$  ( $^3J_{^{15}\text{N}^\alpha\text{C}^\alpha\text{H}}$ ) can be used to determine the dihedral angle  $\psi$  (Wagner, 1990; Gronenborn et al., 1989). Also useful is the three-bond coupling between a backbone  $^{15}\text{N}$  and its own side-chain  $\text{C}^\beta\text{H}$  ( $^3J_{^{15}\text{N}^\alpha\text{C}^\beta\text{H}}$ ), which can be used for stereospecific assignment of  $\beta$ -methylene protons and determination of the dihedral angle  $\chi^1$  (Bystrov, 1976; Wagner, 1990).

Our goal is to study the structure, self-association, and dynamics of alamethicin in the membrane-mimetic environment of a detergent or lipid micelle. In association with detergent or lipid, alamethicin line widths will be considerably broadened, and spectral resolution is expected to degrade. However, an  $^{15}\text{N}$ -labeled alamethicin would have several advantages despite the low intrinsic sensitivity of  $^{15}\text{N}$  ( $\gamma = -2711 \text{ s}^{-1} \text{ G}^{-1}$ ). The low  $\gamma$  results in  $^{15}\text{N}$  resonances which are intrinsically narrower than the  $^1\text{H}$  resonances of the same molecule. Furthermore, the narrower resonance lines, in combination with a greater chemical shift range, result in a significant improvement in spectral resolution compared to protons (Bogusky et al., 1990). If necessary, the resolution of two-dimensional homonuclear proton spectra of  $^{15}\text{N}$ -labeled molecules can be greatly enhanced by spreading out the spectra into a third ( $^{15}\text{N}$ ) dimension (Kay et al., 1990; Clore et al., 1990). Finally, the broad lines and shorter  $T_2$ 's for the peptide in a micelle will reduce the sensitivity of scalar correlation experiments, whereas in an  $^{15}\text{N}$ -labeled molecule the large one-bond coupling between  $^1\text{H}$  and  $^{15}\text{N}$  (90 Hz) and the  $\sin \pi J t$  dependence of magnetization transfer, make the heteronuclear correlation experiment significantly more sensitive (Kay et al., 1990).

The growth requirements for the production of high yields of alamethicins by *T. viride* were systematically optimized by Brewer et al. (1987). They also described growth conditions in which the fungus produces moderate amounts of alamethicins when grown on a basal medium supplemented with inorganic nitrogen. Here, we show that these techniques enable uniform  $^{15}\text{N}$  labeling of alamethicins. The  $^{15}\text{N}$  and  $^1\text{H}$  NMR spectra of an alamethicin are assigned, and the structure and dynamics of the molecule in methanol are discussed in the light of the NMR experiments.

## EXPERIMENTAL PROCEDURES

### Materials

*T. viride* NRLL 3199 and *Micrococcus luteus* (catalogue no. 5337, 381) were purchased from the American type culture collection (Rockville, MD). Fish meal was from Sigma Chemical Co. (St. Louis, MO). Pharmamedia from cotton seed was from Procter and Gamble (Memphis, TN). Molasses and potatoes were purchased from a local grocer. HPLC-grade solvents were from Mallinckrodt (Paris, KY).  $\text{K}^{15}\text{NO}_3$  (99% isotopic purity) and  $^{15}\text{NH}_4\text{Cl}$  (99.5% isotopic purity) were from Isotec Inc. (Miamisburg, OH). The  $\text{CD}_3\text{OD}$  was from Aldrich Chemical Co. (Milwaukee, WI), and  $\text{CD}_3\text{OH}$  was from MSD Isotopes (Pointe Claire, PQ). Other chemicals, minerals, and vitamins were purchased from Fisher Scientific (Fairlawn, NJ), Sigma Chemical Co., and Mallinckrodt. A Beckman (Mississauga, ON) Spherisorb 5- $\mu\text{m}$  C-18 reverse-phase column (10-mm i.d.; 150-mm length) was used for HPLC purification of alamethicin.

### Methods

**Labeling and Purification of Alamethicins.** *T. viride* were cultivated according to the methods of Brewer et al. (1987) with some modifications. The freeze-dried ATCC *T. viride* were cultivated on potato agar petri dishes (ATCC catalogue) (primary culture) and then transferred to malt agar slants and plates (secondary cultures). A small piece of approximately one-week-old fungus was used to inoculate a 20-mL solution containing pharmamedia (0.5 g) and glucose (0.5 g) (tertiary culture). Cultures were grown at 25 °C in an environmental shaker at 100 rpm for 4–5 days. Five milliliters of the culture was used to inoculate 50 mL of a medium containing black

strap molasses (20 g/L), dextrin (3 g/L), fish meal (15 g/L), and pharmedia (15 g/L), adjusted to pH 7 (complex medium) (Meyer & Reusser, 1967). The culture was shaken at 100 rpm and 25 °C for 7 days. After this, the cultures were tested daily for alamethicin production using an antibiotic assay which measured the inhibition of *M. luteus* growth (Brewer et al., 1970). Brewer et al. (1987) point out that alamethicin production by *T. viride* is lost rapidly upon subcultivation; however, we have not observed this so far (18 months) and have not found it necessary to select individual, high-alamethicin-yielding spores for subcultivation.

We obtained good yields of  $^{15}\text{N}$ -labeled alamethicin by modifying the procedures described in Brewer et al. (1987) accordingly: Initially, 5 mL of a seven-day-old *T. viride* culture grown in complex medium (see above) was used to inoculate 50 mL of a medium containing  $\text{K}^{15}\text{NO}_3$  and the vitamins and minerals described in Brewer et al. (1987), except that we substituted 1.5 g of dextrin for the carboxymethylcellulose. This culture was incubated at 25 °C with shaking at 100 rpm for 7 days and then assayed for alamethicin as described above. Only small amounts of  $^{15}\text{N}$ -labeled alamethicin were produced; however, fungi from this preparation were stored frozen and subsequently used to inoculate the  $^{15}\text{N}$ -containing minimal medium which resulted in good yields of  $^{15}\text{N}$ -labeled alamethicin.

After 9–14 days of growth, alamethicin was extracted from the medium using chloroform/methanol as described in Brewer et al. (1987). The organic solvents were removed by rotary evaporation, and the extract was freeze-dried. Alamethicin was then separated into its individual components by HPLC using the conditions given in the legend to Figure 1, which are a modification of those described by Balasubramanian et al. (1981). Triethylammonium acetate and other impurities were removed from the unlabeled protein by recrystallization from boiling acetonitrile.

**NMR Spectroscopy.** HPLC-purified alamethicin was dissolved in 0.55 mL of  $\text{CD}_3\text{OD}$  or  $\text{CD}_3\text{OH}$  to a concentration of 2.4–3.4 mM without adjustment of the pH and placed in a 5-mm NMR tube (Wilmad 535 or 537). The apparent pH was 8.4. There are no ionizable amino acids in the component of alamethicin used in this study (see Results). A DQF-COSY experiment (Marion & Wüthrich, 1983) of alamethicin in  $\text{CD}_3\text{OH}$ , with presaturation of the solvent resonance, was done on a Bruker AM 300 NMR spectrometer equipped with a  $^1\text{H}$ -selective probe head optimized for water suppression. NMR experiments at 500 MHz were done on a Bruker AMX 500 NMR spectrometer using either a 5-mm inverse broadband probe head or a triple-resonance probe head with the inner coil tuned to  $^1\text{H}$  and  $^2\text{H}$  (lock) and the outer coil tuned to  $^{13}\text{C}$  and  $^{15}\text{N}$ . One-dimensional  $^{15}\text{N}$  observe spectra were acquired with and without WALTZ-16 composite pulse  $^1\text{H}$  decoupling during acquisition or during acquisition and the relaxation delay to maintain the NOE. The spin-echo difference experiment (Griffey et al., 1985) was done with  $^{15}\text{N}$  decoupling using the GARP sequence (Shaka et al., 1985) and with presaturation of the solvent resonance. Homonuclear Hartmann-Hahn coherence transfer (TOCSY) was done with the MLEV-17 sequence during a 31-ms isotropic mixing time and with presaturation of the solvent resonance (Bax & Davis, 1985b). The 2D ROESY experiment was run with a cw spin-locking mixing time of 300 ms [see Bax et al. (1986) and Bax and Davis (1985a)] and with presaturation of the solvent resonance. The 2D  $^1\text{H}$ - $^{15}\text{N}$  correlation via heteronuclear zero- and double-quantum coherence (HMQC) was done without decoupling (Bax et al., 1983). All 2D experiments were done

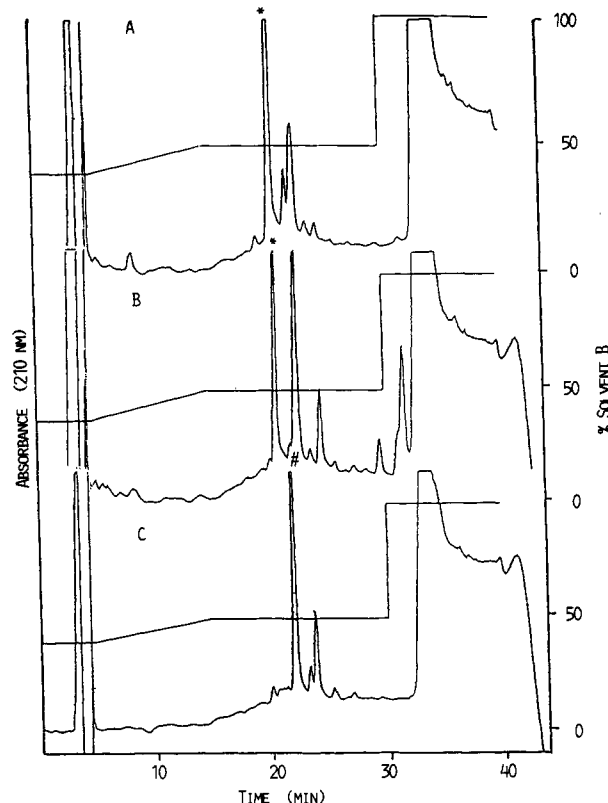


FIGURE 1: HPLC chromatograms of *T. viride* growth medium crude extracts for (A) unlabeled, (B)  $^{15}\text{N}$ -labeled, and (C) Upjohn alamethicins. An asterisk (\*) indicates the peak collected for NMR spectroscopy. A pound sign (#) indicates the major Upjohn alamethicin peak. Samples of 100–500  $\mu\text{L}$  were loaded onto a Beckman Spherisorb 5- $\mu\text{m}$  C-18 reverse-phase column (10-mm i.d.; 150-mm length). (Solvent A) 0.05 N acetic acid adjusted to pH 3.5 with triethylamine. (Solvent B) tetrahydrofuran/acetonitrile/solvent A (8:2:1). Isocratic elution (40% solvent B) was at 1 mL/min for 5 min, followed by a gradient elution at 1.5 mL/min for 10 min to 49% solvent B, followed by isocratic elution at 1 mL/min for 15 min, and finally elution at 1 mL/min for 10 min at 100% solvent B.

in the phase-sensitive mode and used TPPI for quadrature detection (Redfield & Kunz, 1975). The 2D experiments were 512  $t_1$  increments each of 1K data points; data were zero filled in  $F_2$  to 2K and in  $F_1$  to 1K. A  $\pi/2$ -shifted sine-squared filter was applied to  $\omega_1$  and  $\omega_2$  before Fourier transformation, except for the ROESY experiment in which a  $\pi/2$ -shifted sine-bell filter was used. All 2D spectra were baseline corrected by subtracting a 3- or 5-order polynomial from both dimensions. All NMR experiments were done at 300 K, and other details about the acquisitions are given in the legends to the figures.

## RESULTS

**Characterization of  $^{15}\text{N}$ -Labeled Alamethicin.** After 9–14 days of growth on complex medium, 50 mL of *T. viride* culture will yield about 9 mg of unlabeled alamethicin, whereas growth on  $^{15}\text{N}$ -labeling medium usually yields 2–3 mg of  $^{15}\text{N}$ -labeled peptide. Figure 1 compares the HPLC chromatograms for alamethicin extracted from the complex medium (A) and from the  $^{15}\text{N}$ -labeling medium (B), with the preparation provided by Upjohn (C). The complex medium yields minor components at about 21.5 and 22 min and a major one at 20 min which we collected for study by NMR spectroscopy. The  $^{15}\text{N}$ -labeling medium produced the components at 20 and 22 min, but roughly in equal proportions, and an additional minor peak at about 25 min; the  $^{15}\text{N}$ -labeled peak at 20 min was collected for NMR studies. The proportion of each of the components of the extracts is different again in the Upjohn

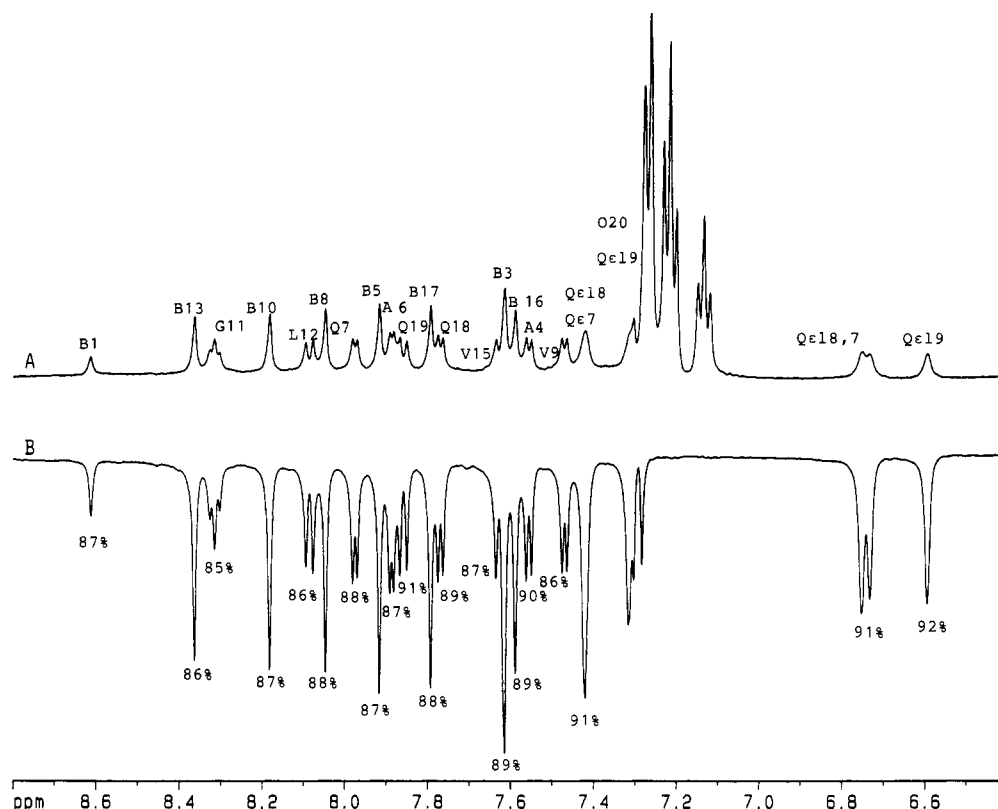


FIGURE 2: Sum (A) and difference (B) of  $^1\text{H}$  NMR spin-echo spectra of  $^{15}\text{N}$ -labeled alamethicin acquired at 500 MHz with and without  $^{15}\text{N}$  population inversion, respectively (Griffey et al., 1985). Peak labels indicate the amino acid (A) and the percent incorporation of  $^{15}\text{N}$  determined by integration of the spectra (B).  $^{15}\text{N}$  was decoupled during the 1.5-s acquisition time using the GARP sequence. A total of 1024 acquisitions were averaged with the recycle delay between acquisitions being 4 s. The internal  $^1\text{H}$  reference was DSS (0 ppm).

extract; the largest component appears at about 22 min, a significant component appears at 25 min, but very little of the 20-min component is observed. Most of the published work on alamethicin to date has used the Upjohn crude preparation or a purified component of it, which presumably corresponds to the peak at 22 min (Figure 1C). Apparently, the peak at 20 min differs from the Upjohn major component by the substitution of a Gln for a Glu at position 18 (see below). According to Brewer et al. (1987), the mixture of peptides produced by the fungus depends upon fermentation conditions such as temperature, pH, age, and aeration.

The extent to which the alamethicin component was enriched by  $^{15}\text{N}$  was determined using spin-echo difference spectroscopy (Griffey et al., 1985). Figure 2 shows the sum (A) and difference (B) of  $^1\text{H}$  NMR spin-echo spectra of  $^{15}\text{N}$ -labeled alamethicin acquired with, and without,  $^{15}\text{N}$  population inversion, respectively (Griffey et al., 1985). Inverting the  $^{15}\text{N}$  puts the attached protons  $180^\circ$  out of phase with respect to the  $^{14}\text{N}$ - and  $^{12}\text{C}$ -attached protons, with the result that the  $^{15}\text{N}$ -attached resonances cancel when the spectra are added (A), and all other resonances cancel when the spectra are subtracted (B). For protons at 500 MHz, the resolution in one-dimensional spectra makes it possible to determine, by integration, the isotopic content at nearly every nitrogen site in the protein except the prolines. The percent incorporation of  $^{15}\text{N}$  at each site is indicated under the peaks in Figure 2B. The peak assignments are indicated above the peaks in Figure 2A, and these were determined as described below. The incorporation of  $^{15}\text{N}$  was uniform throughout the sites ranging from 85% to 92%. Figure 2 also illustrates a line-narrowing effect of  $^{15}\text{N}$  on the directly attached protons compared to the  $^{14}\text{N}$ -attached protons. This is due mainly to the difference in heteronuclear dipolar coupling between the

two isotopes of nitrogen (Llinas et al., 1978; Bax et al., 1989).

**Assignment of  $^1\text{H}$  Resonances.** Since the  $^1\text{H}$  NMR resonances of the alamethicin component at 22 min (Figure 1) have been assigned (Davis & Gisin, 1981; Banerjee et al., 1983; Esposito et al., 1987) and since the sequence of the peptide at 20 min differs only slightly from it, we present just a brief outline of our assignment strategy. The three amide singlet resonances, which appear between 6.5 and 6.8 ppm in one-dimensional  $^1\text{H}$  NMR spectra of the peptide in methanol (Figure 2), suggest the presence of three residues with primary amide side chains; in contrast, the previously assigned alamethicin contains only two such residues. Figure 2 also shows the presence of eight Aib singlet amide resonances, a single Gly amide triplet (8.33 ppm), and the aromatic resonances from a single Pho (7.1–7.3 ppm). This spectrum, and a DQF-COSY experiment at 300 MHz (not shown), confirmed that the amino acid composition of the isolated component is identical to that of the component at 22 min in Figure 1 except for the replacement of a Glu by a Gln at one site. The spin system assignment was completed with a TOCSY spectrum acquired at 500 MHz (Figure 3). For illustration, the continuous lines in Figure 3 show the complete spin systems for the two prolines, the two alanines, and the phenylalaninol. No cross peaks between the Aib methyls and their amides are observed in correlation spectra (Figure 3) because of the small four-bond coupling between them. Thus, Aib methyls were assigned using the ROESY experiment and heteronuclear  $^1\text{H}/^{15}\text{N}$  correlations (see below).

One method of sequential assignment of amino acid spin systems relies on NOE connectivities between neighboring spin systems in the amino acid sequence (Wüthrich, 1986). A NOESY spectrum of unlabeled alamethicin in  $\text{CD}_3\text{OH}$  at 300 MHz produced very few cross peaks, and 1D NOE difference

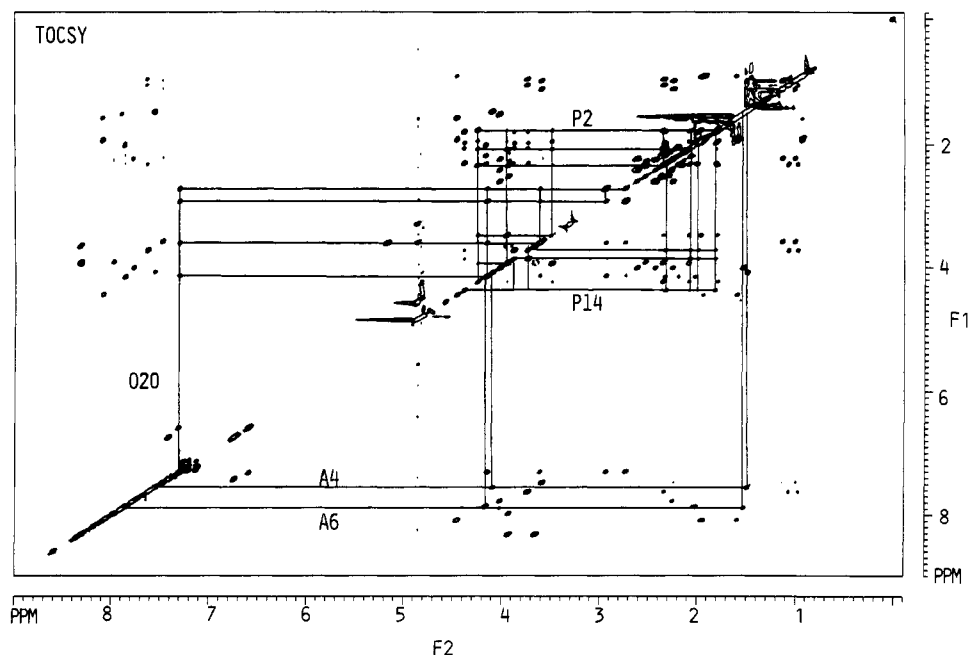


FIGURE 3: Complete TOCSY spectrum at 500 MHz of unlabeled alamethicin. The spin systems for the two prolines, two alanines, and the phenylalaninol are indicated by continuous lines. The internal  $^1\text{H}$  reference was DSS (0 ppm). The number of scans was 64 for each of 512 increments.

Table I:  $^{15}\text{N}$  and  $^1\text{H}$  Chemical Shifts (ppm) of Alamethicin in Methanol ( $\text{CD}_3\text{OH}$ ) at 27  $^\circ\text{C}^a$

residue	$^{15}\text{N}$	NH	$\text{C}^\alpha\text{H}$	$\text{C}^\beta\text{H}$	others
B1	138.7	8.61		1.46, 1.54	<i>N</i> -acetyl $\text{CH}_3$ 2.05
P2	(132.3) (131.0)		4.24	2.34, 1.79	$\text{C}^\gamma\text{H}$ 2.07; $\text{C}^\gamma\text{H}$ 1.95; $\text{C}^\delta\text{H}$ 3.49; $\text{C}^\delta\text{H}$ 3.95
B3	126.0	7.62		1.54	
A4	118.9	7.56	4.09	1.49	
B5	129.5	7.92		1.48, 1.55	
A6	117.2	7.90	4.02	1.52	
Q7	118.6 $\text{N}^a$ 107.9	7.98	3.92	2.28, 2.15	$\text{C}^\gamma\text{H}$ 2.53; $\text{C}^\gamma\text{H}$ 2.36; $\text{N}^a\text{H}_2$ 7.42; $\text{N}^a\text{H}_E$ 6.74
B8	129.22	8.06		1.59, 1.52	
V9	115.5	7.48	3.58	2.23	$\text{C}^\gamma\text{H}_3$ 1.13; $\text{C}^\gamma\text{H}_3$ 0.99
B10	131.4	8.20		1.56	
G11	101.7	8.22	3.93, 3.67		
L12	119.6	8.09	4.46	1.92, 1.59	$\text{C}^\gamma\text{H}$ 1.92; $\text{C}^\delta\text{H}$ 0.94; $\text{C}^\delta\text{H}$ 0.91
B13	134.7	8.38		1.61, 1.53	
P14	(132.3) (131.0)		4.38	2.31, 1.80	$\text{C}^\gamma\text{H}$ 2.07; $\text{C}^\gamma\text{H}$ 1.98; $\text{C}^\delta\text{H}$ 3.87; $\text{C}^\delta\text{H}$ 3.73
V15	117.0	7.63	3.73	2.32	$\text{C}^\gamma\text{H}_3$ 1.07; $\text{C}^\gamma\text{H}_3$ 0.96
B16	131.0	7.59		1.55, 1.50	
B17	126.0	7.80		1.53	
Q18	114.8, $\text{N}^a$ 108.1	7.78	4.02	2.23	$\text{C}^\gamma\text{H}$ 2.62; $\text{C}^\gamma\text{H}$ 2.43; $\text{N}^a\text{H}_2$ 7.42; $\text{N}^a\text{H}_E$ 6.76
Q19	116.9, $\text{N}^a$ 107.8	7.87	4.16	2.02	$\text{C}^\gamma\text{H}$ 2.53; $\text{C}^\gamma\text{H}$ 2.36; $\text{N}^a\text{H}_2$ 7.31; $\text{N}^a\text{H}_E$ 6.60
O20	120.8	7.29	4.14	2.94, 2.73	$\text{C}^\beta\text{H}_2$ 3.61; $\text{C}^\beta\text{H}$ 7.20; $\text{C}^\beta\text{H}$ 7.28; $\text{C}^\beta\text{H}$ 7.14

<sup>a</sup> The internal  $^1\text{H}$  reference was DSS (0 ppm). The external  $^{15}\text{N}$  reference was 2.9 M  $^{15}\text{NH}_4\text{Cl}$  in 1 M HCl, which resonates at 24.93 ppm with respect to liquid  $\text{NH}_3$  (Levy & Lichter, 1979). <sup>b</sup> The Pro  $^{15}\text{N}$  resonances have not been sequentially assigned.

spectroscopy, in which several of the well-resolved amides were saturated, did not produce any enhancements (not shown). The theoretical intensity of the maximum transient NOE at 300 MHz is plotted as a function of  $\tau_c$  in Figure 4 (---), and the lack of NOE may be used to estimate a  $\tau_c$  of about 0.3 ns, for alamethicin at 300 K in methanol. Figure 4 also illustrates that increasing the field to 500 MHz (---), would result in a small, negative, transient NOE. However, the transient NOE measured in the rotating frame at 500 MHz (---) is nearly 3 times larger, and for this reason we used the ROESY experiment (Figure 5) (Bothner-By et al., 1984) to make sequential assignments in alamethicin.

Sequential  $^1\text{H}$  assignments for alamethicin are listed in Table I. Glycine, leucine, and phenylalaninol occur only once in the peptide, so identification of their spin systems allowed sequential assignment to Gly-11, Leu-12, and Pho-20. A cross peak between the amide protons of Gly-11 and Leu-12 occurs near the end of a stretch of seven  $\text{NH}(i)\text{--NH}(i+1)$  connec-

tivities between Ala-6 and Aib-13 (see Figure 5A). Also connected by  $\text{NH}(i)\text{--NH}(i+1)$  were residues 3, 4, and 5, residues 15, 16, and 17, and residues 18 and 19 (see Figures 5A and 6). The cross peak connecting the amides of residues 19 and 20 is ambiguous owing to the overlap of the Pho-20 NH and the Pho-20 2,6 ring protons. Sequential assignment of the two proline residues, and Aibs 1 and 3, relied on ROESY connectivities between the amide of an assigned residue and the side chains and  $\text{C}^\alpha\text{H}$  of a preceding residue (see Figure 5B). The ROESY experiment also allowed unambiguous assignment of the three glutamine  $\text{N}^a\text{H}_2$ 's to their respective residues and confirmed the replacement of Glu-18 by a Gln residue in the isolated component of alamethicin. However, the ROESY experiment done in  $\text{CD}_3\text{OH}$  could not be used to unambiguously assign the phenylalaninol 2,6 and 3,5 ring protons due to overlap with the amide of the phenylalaninol and the syn  $\text{N}^a\text{H}$  of Gln-19 (see Figure 5). This assignment was made by acquiring a ROESY spectrum in

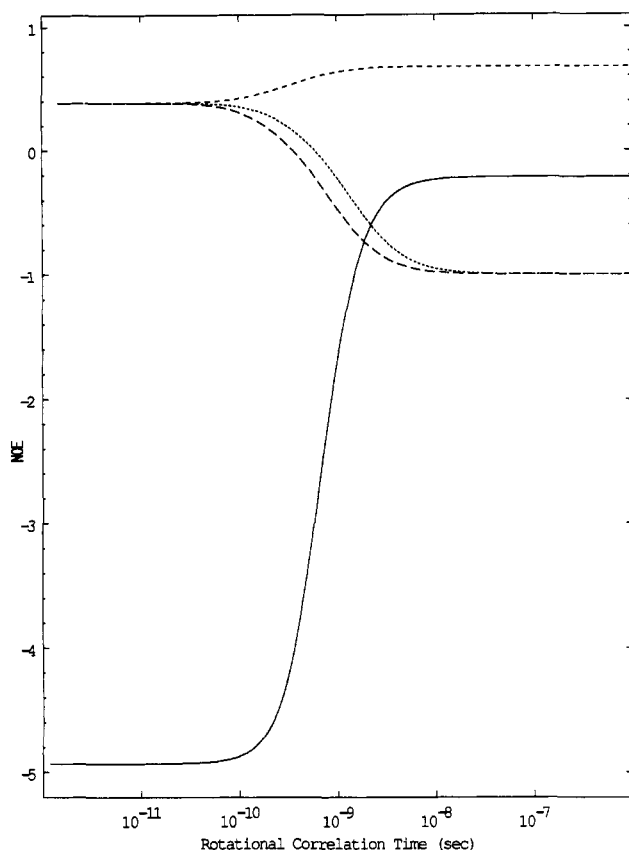


FIGURE 4: The dependence of various maximum NOEs on rotational correlation time ( $\tau_c$ ); the maximum transient homonuclear  $^1\text{H}\{^1\text{H}\}$  NOEs at 500.13 MHz (---) and 300.13 MHz (....); the maximum transient rotating frame homonuclear  $^1\text{H}\{^1\text{H}\}$  NOE at 500.13 MHz (-.-.); and the maximum heteronuclear  $^{15}\text{N}\{^1\text{H}\}$  NOE (—) at 500.13 MHz for  $^1\text{H}$  and 50.68 MHz for  $^{15}\text{N}$ . Calculated from the equations given in Neuhaus and Williamson (1989). See also Kay et al. (1989) and Bothner-Bj et al. (1984).

$\text{CD}_3\text{OD}$  in which the labile amide protons were exchanged out (not shown).

It is worth noting that Table I includes a few stereospecific assignments. One disadvantage of the ROESY experiment is that various types of direct and indirect coherence transfer can appear, including peaks connecting spins in different coupling networks (Neuhaus & Williamson, 1989; Clore et al., 1991). Spin system assignment should not be affected by the contributions to ROESY cross peaks from intrasidue coherence transfer. Likewise, interresidue ROESY cross peaks will not contain a coherence transfer component unless there is also an NOE connection between the spin systems, and this is unlikely to lead to incorrect secondary structure determination. However, stereospecific assignment of  $\beta$ -methylene protons, the prochiral protons of the prolines, and the Aib methyls relies on differences in intensities of intrasidue NOE cross peaks (Wüthrich, 1986; Esposito et al., 1987) and could be misinterpreted if coherence transfer were present. Less problematic is the stereospecific assignment of the proline peptide bonds. Interresidue NOEs between  $\text{NH}_i$  and  $\text{Pro-}\delta_{i+1}$  (Figure 5B), and the absence of ( $\text{NH}_i$ ,  $\text{Pro-}\alpha_{i+1}$ ) and ( $\alpha_i$ ,  $\text{Pro-}\alpha_{i+1}$ ) cross peaks, support a trans configuration (Wüthrich, 1986) at both sites, in agreement with the NMR results of Esposito et al. (1987). The assignment of the glutamine amide resonances is based on the observation that the  $\text{H}_Z$  (syn) substituent almost always resonates at a higher field than the  $\text{H}_E$  (anti) substituent (Perrin et al., 1980).

A summary of the short- and medium-range NOE connectivities is given in Figure 6. Also listed are the intrasidue

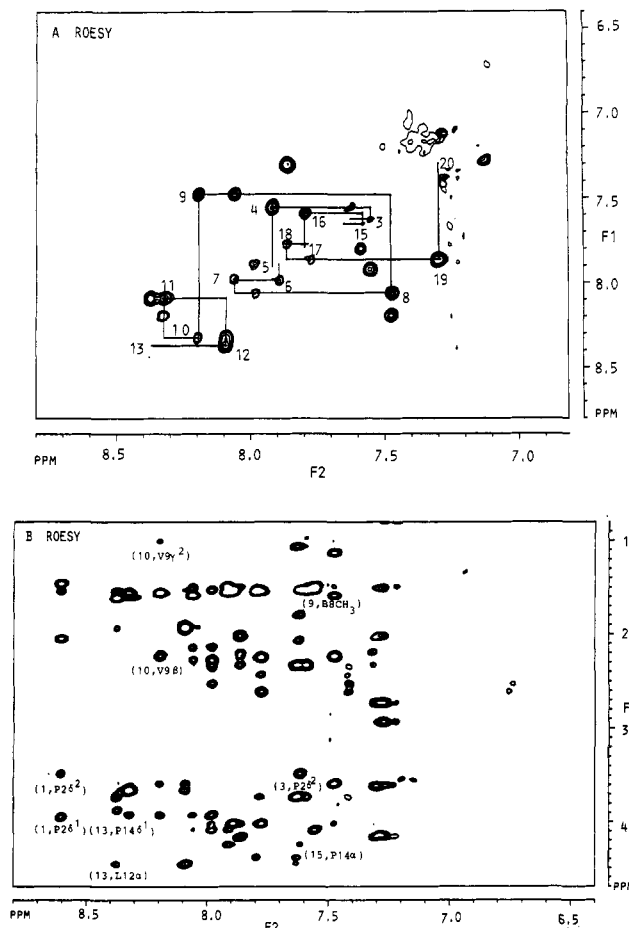


FIGURE 5: (A) NH-NH region of a 300-ms mixing time ROESY spectrum of unlabeled alamethicin in  $\text{CD}_3\text{OH}$  acquired at 500 MHz.  $\text{NH}(i)$ - $\text{NH}(i+1)$  connectivities between residues 3-5, 6-13, 15-17, and 18-20 are indicated by continuous lines. (B) NH/aromatic-aliphatic region of the same spectrum as in panel A above. A few interresidue cross peaks are labeled. The internal  $^1\text{H}$  reference was DSS (0 ppm).

$J_{\alpha\text{N}}$  and  $J_{\alpha\beta}$  coupling constants which contain information about the configuration about the dihedral angles  $\phi$  and  $\chi_1$ , respectively. The  $J_{\alpha\text{N}}$  were most conveniently measured from the  $^1\text{H}$  spectrum of  $^{15}\text{N}$ -labeled alamethicin because of the improved resolution in the amide region (see Figure 2B). More difficult to measure are the  $J_{\alpha\beta}$  coupling constants. Where these are large, they could be measured from the cross peaks in the DQF-COSY spectrum (not shown); however, the  $J_{\alpha\beta}$  for only four residues could be measured in this way.

**Assignment of  $^{15}\text{N}$  Resonances.** The correlation of  $^1\text{H}$  with their directly bonded  $^{15}\text{N}$ , in uniformly  $^{15}\text{N}$ -labeled alamethicin (Figure 7), was done using the heteronuclear zero- and double-quantum coherence experiment (HMQC) of Bax et al. (1983). Since the protons had already been assigned, the assignment of the  $^{15}\text{N}$  resonances was straightforward, and these are listed in Table I. Figure 7A also shows the chemical shift ranges of the different amino acids; all eight Aib  $^{15}\text{N}$  resonances occur in a group between 125 and 140 ppm. Upfield of these, between 114 and 120 ppm, are the rest of the backbone  $^{15}\text{N}$  resonances except the glycine  $^{15}\text{N}$ . Upfield of the backbone amides are the three Gln side-chain amides, at about 108 ppm. The Gly-11  $^{15}\text{N}$  resonance is the most upfield-shifted nitrogen, resonating at 101 ppm. This pattern of chemical shifts is a result of the "β effect" in which the secondary  $^{15}\text{N}$  amide resonances are increasingly deshielded by the addition of one (e.g., Ala) or two (Aib) β substituents and is a well-documented observation in  $^{13}\text{C}$  (Breitmaier &

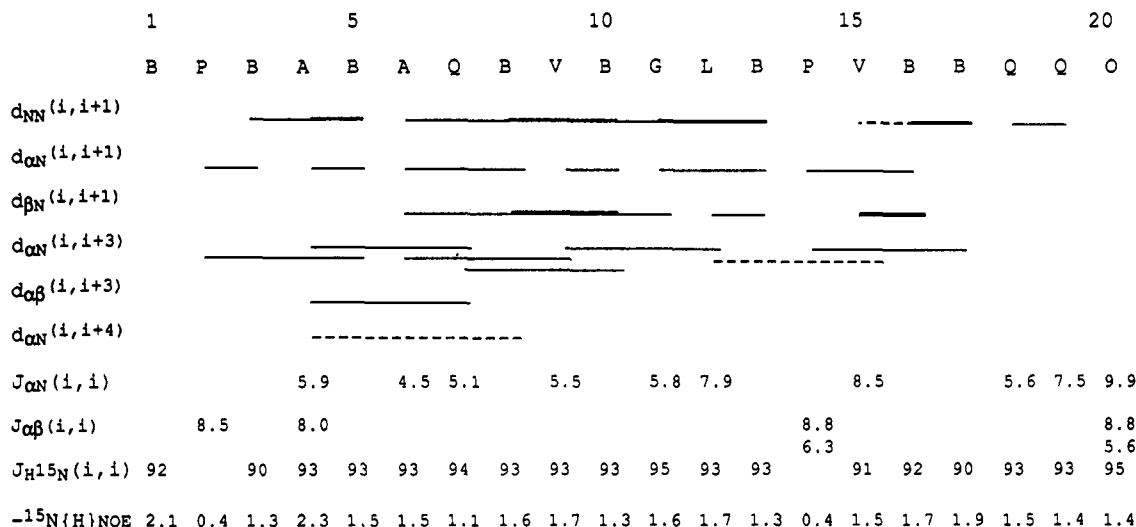


FIGURE 6: Amino acid sequence of alamethicin with a summary of the short- and medium-range rotating frame NOE connectivities, homonuclear and heteronuclear scalar coupling constants, and heteronuclear  $\{^1\text{H}\}^{15}\text{N}$  NOEs. The heavy, light, and dashed lines indicate strong, medium, and weak NOEs, respectively.

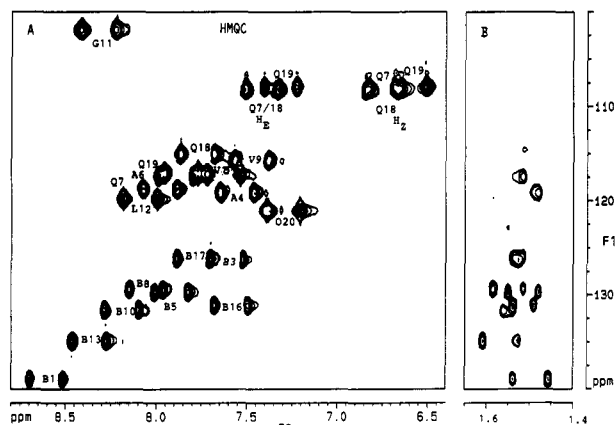


FIGURE 7: (A)  $^{15}\text{N}$ - $^1\text{H}$  region of a  $^{15}\text{N}$ - $^1\text{H}$  HMQC spectrum of uniformly  $^{15}\text{N}$ -labeled alamethicin in  $\text{CD}_3\text{OH}$  acquired at 500 MHz illustrating the assignments of all  $^{15}\text{N}$  resonances of alamethicin except the prolines. (B)  $^{15}\text{N}$ - $\text{CH}_3$  region of the same spectrum as in panel A used to assign the Aib methyls. The internal  $^1\text{H}$  reference was DSS (0 ppm). The external  $^{15}\text{N}$  reference was  $2.9\text{ M } ^{15}\text{NH}_4\text{Cl}$  in  $1\text{ M HCl}$ , which resonates at 24.93 ppm with respect to liquid  $\text{NH}_3$  (Levy & Lichter, 1979). The number of scans was 128 for each of 512 increments.

Voelter, 1987) and  $^{15}\text{N}$  (Westerman & Roberts, 1978) NMR of organic molecules.

Despite the fact that the heteronuclear experiment was optimized for a heteronuclear coupling of 90 Hz, three-bond correlations to the  $C^{\delta}H_3$  of the Aib and Ala residues are observable in Figure 7. Presumably, the large number of scans (128), the intensities of the methyls, and the magnitude of their  $^3J$  coupling to the  $^{15}N$  allow enough antiphase magnetization to grow during the short  $1/(2J)$  period to be converted into detectable zero- and double-quantum coherences. These correlations allowed unambiguous assignment of all previously unassigned Aib methyls. These assignments proved useful since they allowed identification of some ROESY cross peaks between Aib methyls and neighboring amino acid amides and side chains.

Since the HMQC experiment shown in Figure 7 was done without  $^1\text{H}$  decoupling, the  $^1J_{\text{S-NH}}$  coupling constants could be measured, and these are listed in Figure 6. Most of these measurements could also be confirmed in the coupled 1D  $^1\text{H}$  NMR spectrum of the  $^{15}\text{N}$ -labeled molecule (not shown). All of the coupling constants occur in the narrow range from 90

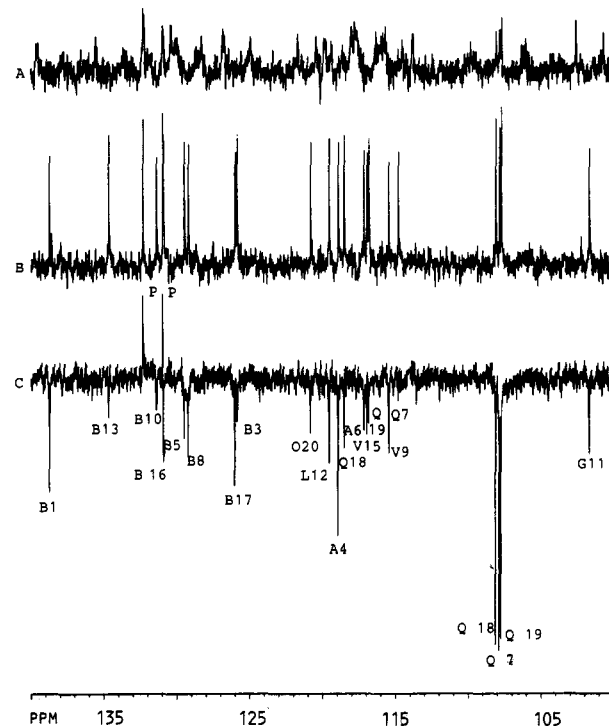


FIGURE 8:  $^{15}\text{N}$  NMR spectra of labeled alamethicin acquired at 500 MHz (A) without  $^1\text{H}$  decoupling, (B)  $^1\text{H}$  decoupled without NOE, and (C)  $^1\text{H}$  decoupled with NOE. Each experiment was the average of 21 120 acquisitions each of 0.8 s. The recycle delay was 10 s. Protons were decoupled using WALTZ-16. The external reference was  $2.9\text{ M } ^{15}\text{NH}_4\text{Cl}$  in  $1\text{ M HCl}$ , which resonates at 24.93 ppm with respect to liquid  $\text{NH}_3$ .

to 95 Hz, which is characteristic of trigonal bonding at the nitrogen. In small molecules, a  $^1J_{\text{NH}}$  in the vicinity of 75 Hz indicates pyramidal bonding, whereas a  $^1J_{\text{NH}}$  of 135 Hz indicates a linear bonding at the nitrogen (Levy & Lichter, 1979). Several attempts have been made to correlate the  $^1J_{\text{NH}}$  with the dihedral angle  $\omega$  (Sogn et al., 1973); however, this has not yet been found useful in protein structure determinations (McIntosh et al., 1990).

**Peptide Dynamics.** Despite the high content of  $^{15}\text{N}$  in the labeled protein, direct observation of  $^{15}\text{N}$  is a time-consuming experiment because of the low  $\gamma$ . Figure 8A shows an  $^{15}\text{N}$  spectrum of labeled alamethicin without proton decoupling.



After 21 120 scans, the signal to noise ratio is very low.  $^1\text{H}$  decoupling during the acquisition period enhances the intensities of the  $^{15}\text{N}$  resonances as shown in Figure 8B. This direct detection of  $^{15}\text{N}$  enabled the observation of the two Pro resonances (at 131 and 132.3 ppm) which are not detectable in the HMQC experiment (Figure 7) because of the lack of directly bonded protons. In these experiments, the long relaxation delay (10 s) allowed any NOE, which might have built up during the acquisition period, to decay. This was checked by doing an experiment with a 20-s delay. Maintaining the NOE by irradiation of  $^1\text{H}$  during the relaxation delay provides information about the dynamics of different  $^{15}\text{N}$  sites in the molecule (Figure 8C). The maximum  $^{15}\text{N}\{^1\text{H}\}$  steady-state NOE ranges from -4.9, for rapidly reorienting sites, to -0.2, for more constrained sites, and is a sensitive indicator of protein dynamics (see Figure 4, solid line; Bogusky et al., 1990; Kay et al., 1989). As expected, the most negative NOEs are those of the side chains of the three Gln residues, an indication that these are the least conformationally constrained of the  $^{15}\text{N}$  atoms. The only positive signals observed were those of the two Pro residues. Assuming that the  $^{15}\text{N}$  is relaxed primarily by dipolar coupling [see Llinas and Wüthrich (1978)], this suggests that the prolines contain the most conformationally restricted nitrogens. Apart from Gln-7, for which the NOE is exactly -1, cancelling the signal, the rest of the backbone amides display a range of negative intensities. A summary of the heteronuclear NOE intensities is listed in Figure 6.

## DISCUSSION

Figure 6 presents a summary of the structural and dynamic properties of alamethicin dissolved in methanol as determined by  $^1\text{H}$  and  $^{15}\text{N}$  NMR spectroscopies. The measured  $^3J_{\text{NHC}^{\alpha}\text{H}}$  for residues Ala-4–Gly-11 are all less than 6 Hz, indicating a helical conformation in the N-terminus of the molecule. The  $d_{\text{NN}}(i,i+1)$ ,  $d_{\alpha\text{N}}(i,i+3)$ ,  $d_{\alpha\beta}(i,i+3)$ , and  $d_{\alpha\text{N}}(i,i+4)$  NOEs [see Wüthrich (1986)] support the conclusion that the peptide in methanol is helical between Ala-4 and Gly-11 (Banerjee et al., 1983; Esposito et al., 1987). Additionally, the  $d_{\alpha\text{N}}(i,i+3)$  connecting Pro-2 and Aib-5 suggests that the helix may extend to Pro-2. These results are in good agreement with the findings of Esposito et al. (1987). In the N-terminus (up to Gly 11) of Glu-18 alamethicin, they detected three  $d_{\alpha\text{side chain}}(i,i+3)$  NOEs, one  $d_{\alpha\text{N}}(i,i+3)$  NOE, and seven  $d_{\text{NN}}(i,i+1)$  NOEs using the NOESY experiment at -5 °C in methanol.

The NMR data are less conclusive about the conformation of the C-terminus of alamethicin (Leu-12–Pho-20). As pointed out in the introduction, this is, at least in part, due to the lack of  $\text{C}^{\alpha}\text{H}$  resonances for the three Aibs and the absence of an NH resonance for Pro-14. Thus, in the C-terminus we detected only one medium intensity and one very weak  $d_{\alpha\text{N}}(i,i+3)$  NOE, using ROESY. Esposito et al. (1987) detected one  $d_{\alpha\text{side chain}}(i,i+3)$  NOE in the last nine residues using NOESY. Also, the  $d_{\text{NN}}(i,i+1)$  connectivity is broken between Aib-17 and Gln-18 and is very weak between Val-15 and Aib-16. Furthermore, of the five measurable  $^3J_{\text{NHC}^{\alpha}\text{H}}$  only the coupling constant for Gln-18 (5.6 Hz) corresponds to a value normally found for helices. The  $^3J_{\text{NHC}^{\alpha}\text{H}}$  for Leu-12, Val-15, and Gln-19 are all in the range of 7.5–8.5 Hz, characteristic of conformational averaging (Bystrov, 1976; Kaptein, 1988). The 9.9-Hz coupling constant for Pho-20 suggests that the peptide backbone is in an unfolded or extended conformation at its C-terminus (Dyson & Wright, 1991). These results suggest the possibility that the lack of NOEs in the C-terminus may be partly due to dynamic averaging of the structure.

In the crystals of alamethicin used for X-ray diffraction, the asymmetric unit contains three independent molecules (Fox

& Richards, 1982). The backbone conformations of residues 1–10 are nearly identical in each of the three molecules. Beyond residue 10, however, the molecules show increasing differences in conformation, particularly for the last three amino acids. The possibility that the C-terminus can exist in more than one conformation in solution gains further support from the molecular dynamics simulations of Fraternali (1990). The simulations suggest that large conformational transitions can occur at positions 11, 12, 15, 18, and 19. However, it is also possible that one or more of the coupling constants in the range of 7.5–8.5 Hz indicate deviations from the standard helical conformation rather than dynamic averaging of structures. For example, a bend in the helix near Leu-12 might account for its  $^3J_{\text{NHC}^{\alpha}\text{H}}$  value. The measurement of additional NMR structural constraints should permit us to distinguish between these possibilities.

Davis and Gisin (1981) obtained evidence for conformational flexibility of the C-terminus of alamethicin from measurements of backbone amide hydrogen exchange rates [for reviews, see Englander and Kallenbach (1984) and Gregory and Rosenberg (1986)]. They classified amide exchange rates from alamethicin dissolved in  $\text{CD}_3\text{OD}$  into a very slowly exchanging group in the segment Aib-3–Aib-10 and a slowly exchanging group from Gly-11 to Aib-16. These results agree generally with the results deduced from molecular dynamics (Fraternali, 1990). The heteronuclear  $^{15}\text{N}\{^1\text{H}\}$  NOE also depends on the local dynamics of the peptide, but there is no obvious correlation between this NOE (see Figures 6 and 8) and the previously measured hydrogen exchange rates. Thus, the high frequency motions ( $10^8$ – $10^{12}$  s $^{-1}$ ) which determine the heteronuclear NOEs appear not to influence the hydrogen exchange rates, which are governed by motions occurring on a much slower time scale ( $<10^6$  s $^{-1}$ ). The heteronuclear NOE cannot confirm the local dynamics of the molecule determined by the molecular dynamics simulations ( $10^{10}$ – $10^{12}$  s $^{-1}$ ), which is somewhat surprising in view of the similar range of time scales of the two experiments.

The availability of uniform  $^{15}\text{N}$ -labeled alamethicin should permit a more precise determination of the structure and dynamics in methanol, particularly of the carboxyl terminus, by increasing the number of measured constraints [see Wagner (1990)]. The putative conformational flexibility of the C-terminus of alamethicin could play a role in membrane insertion of the peptide, ion pore formation, or properties of the channels such as the voltage-gating mechanism. Thus, it will be of interest to determine the effects of detergent and lipid on both the structure and dynamics of the peptide.  $^{15}\text{N}$  NMR has proven to be a particularly valuable tool in measurements of the structure (Henry & Sykes, 1990a) and dynamics (Henry & Sykes, 1990b) of another detergent-solubilized membrane protein the M13 coat protein.

## ACKNOWLEDGMENTS

We thank Dr. Floyd Kapeki of Upjohn (Kalamazoo, MI) for the *T. viride* extract. We are grateful to Mr. Kirk Marat and Dr. Sandra Mooibroek (Bruker Canada) for helpful advice on spectrometer operation and to Mr. Marat and Mr. Terry Wolowiec for maintaining the NMR spectrometers.

## REFERENCES

- Anderson, O. A. (1984) *Annu. Rev. Physiol.* **46**, 531–548.
- Balasubramanian, T. M., Kendrick, N. C. E., Taylor, M., Marshall, G. R., Hall, J. E., Vodyanoy, I., & Reusser, F. (1981) *J. Am. Chem. Soc.* **103**, 6127–6132.
- Banerjee, U., & Chan, S. I. (1983) *Biochemistry* **22**, 3709–3713.



- Banerjee, U., Tsui, F.-P., Balasubramanian, T. N., Marshall, G. R., & Chan, S. I. (1983) *J. Mol. Biol.* 165, 757-775.
- Bax, A., & Davis, D. G. (1985a) *J. Magn. Reson.* 63, 207-213.
- Bax, A., & Davis, D. G. (1985b) *J. Magn. Reson.* 65, 355-360.
- Bax, A., Griffey, R. H., & Hawkins, B. L. (1983) *J. Magn. Reson.* 55, 301-315.
- Bax, A., Sklenar, V., & Summers, M. F. (1986) *J. Magn. Reson.* 70, 327-331.
- Bax, A., Sparks, S. W., & Torchia, D. A. (1988) *J. Am. Chem. Soc.* 110, 7926-7927.
- Bax, A., Kay, L. E., Sparks, S. W., & Torchia, D. A. (1989) *J. Am. Chem. Soc.* 111, 408-409.
- Bogusky, M. J., Leighton, P., Schiksnis, R. A., Khoury, A., Lu, P., & Opella, S. J. (1990) *J. Magn. Reson.* 86, 11-29.
- Bothner-By, A. A., Stephens, R. L., Lee, J.-M., Warren, C. D., & Jeanloz, R. W. (1984) *J. Am. Chem. Soc.* 106, 811-813.
- Breitmaier, E., & Voelter, W. (1987) *Carbon-13 NMR Spectroscopy*, 3rd ed., VCH Publishers, New York.
- Brewer, D., Jerram, W. A., Meiler, D., & Taylor, A. (1970) *Can. J. Microbiol.* 16, 433-440.
- Brewer, D., Mason, F. G., & Taylor, A. (1987) *Can. J. Microbiol.* 33, 619-625.
- Bystrov, V. F. (1976) *Prog. Nucl. Magn. Reson. Spectrosc.* 10, 41-81.
- Bystrov, V. F., Gavrilov, Y. D., Ivanov, V. T., & Ovchinnikov, Y. A. (1977) *Eur. J. Biochem.* 78, 63-82.
- Clore, G. M., Driscoll, P. C., Wingfield, P. T., & Gronenborn, A. M. (1990) *Biochemistry* 29, 7387-7401.
- Clore, G. M., Bax, A., & Gronenborn, A. M. (1991) *J. Biomol. NMR* 1, 13-22.
- Davis, D. G., & Gisin, B. F. (1981) *FEBS Lett.* 133, 247-251.
- Dyson, H. J., & Wright, P. E. (1991) *Annu. Rev. Biophys. Biophys. Chem.* 20, 519-538.
- Eisenberg, M., Hall, J. E., & Mead, C. A. (1973) *J. Membr. Biol.* 14, 143-176.
- Englander, S. W., & Kallenbach, N. R. (1984) *Q. Rev. Biophys.* 16, 521-655.
- Esposito, G., Carver, J. A., Boyd, J., & Campbell, I. D. (1987) *Biochemistry* 26, 1043-1050.
- Fox, R. O., & Richards, F. M. (1982) *Nature* 300, 325-330.
- Fraternali, F. (1990) *Biopolymers* 30, 1083-1099.
- Gisin, B. F., Davis, D. G., Borowska, Z. K., Hall, J. E., & Kobayashi, S. (1981) *J. Am. Chem. Soc.* 103, 6373-6377.
- Gregory, R. B., & Rosenberg, A. (1986) *Methods Enzymol.* 131, 448-508.
- Griffey, R. H., Redfield, A. G., Loomis, R. E., & Dahlquist, F. W. (1985) *Biochemistry* 24, 817-822.
- Gronenborn, A. F., Wingfield, P. T., & Clore, G. M. (1989) *Biochemistry* 28, 5081-5089.
- Hall, J. E., Vodyanov, I., Balasubramanian, T. M., & Marshall, G. M. (1984) *Biophys. J.* 45, 233-247.
- Henry, G. D., & Sykes, B. D. (1990a) *J. Mol. Biol.* 212, 11-14.
- Henry, G. D., & Sykes, B. D. (1990b) *Biochemistry* 29, 6303-6313.
- Jen, W.-C., Jones, G. A., Brewer, D., Parkinson, V. O., & Taylor, A. (1987) *J. Appl. Bacteriol.* 63, 293-298.
- Karle, I., & Balaram, P. (1990) *Biochemistry* 29, 6747-6761.
- Kay, L. E., Torchia, D. A., & Bax, A. (1989) *Biochemistry* 28, 8972-8979.
- Kay, L. E., Clore, G. M., Bax, A., & Gronenborn, A. M. (1990) *Science* 249, 411-414.
- Kay, L. E., Ikura, M., Tschudin, R., & Bax, A. (1990) *J. Magn. Reson.* 89, 496-514.
- Latore, R., Miller, C. G., & Quay, S. (1981) *Biophys. J.* 36, 803-809.
- Levy, G. C., & Lichter, R. L. (1979) *Nitrogen-15 Nuclear Magnetic Resonance Spectroscopy*, John Wiley and Sons, Toronto.
- Llinas, M., & Wüthrich, K. (1978) *Biochim. Biophys. Acta* 532, 29-40.
- Llinas, M., Klein, M. P., & Wüthrich, K. (1978) *Biophys. J.* 24, 849-862.
- Marion, D., & Wüthrich, K. (1983) *Biochem. Biophys. Res. Commun.* 113, 967-974.
- Marshall, G. R., Hodgkin, E. E., Langs, D. A., Smith, G. D., Zabrocki, J., & Leplawy, M. T. (1990) *Proc. Natl. Acad. Sci. U.S.A.* 87, 487-491.
- Mathew, M. K., Nagaraj, R., & Balaram, P. (1981) *Biochem. Biophys. Res. Commun.* 98, 548-555.
- McIntosh, L. P., Wand, A. J., Lowry, D. F., Redfield, A. G., & Dahlquist, F. W. (1990) *Biochemistry* 29, 6341-6362.
- Meyer, C. E., & Reusser, F. (1967) *Experientia* 23, 85-86.
- Neuhaus, D., & Williamson, M. (1989) *The Nuclear Overhauser Effect in Structural and Conformational Analysis*, VCH Publishers, New York.
- Perrin, C. L., Johnston, E. R., & Ramirez, J. L. (1980) *J. Am. Chem. Soc.* 102, 6299-6304.
- Redfield, A. G., & Kunz, S. D. (1975) *J. Magn. Reson.* 63, 250-254.
- Reusser, F. (1967) *J. Biol. Chem.* 243-247.
- Rindfleisch, H., & Kleinkauf, H. (1976) *FEBS Lett.* 62, 276-280.
- Shaka, A. J., Barker, P. B., & Freeman, R. (1985) *J. Magn. Reson.* 64, 547.
- Sogn, J. A., Gibbons, W. A., & Randall, E. W. (1973) *Biochemistry* 12, 2100-2105.
- Stockman, B. J., Westler, W. M., Mooberry, E. S., & Markley, J. L. (1988) *Biochemistry* 27, 136-142.
- Tosteson, M. T., & Tosteson, D. (1982) *Biophys. J.* 36, 109-116.
- Wagner, G. (1990) *Prog. Nucl. Magn. Reson. Spectrosc.* 22, 101-139.
- Westerman, P. W., & Roberts, J. D. (1978) *J. Org. Chem.* 43, 1177-1179.
- Wüthrich, K. (1986) *NMR of Proteins and Nucleic Acids*, John Wiley, New York.
- Zagorski, M. G., Norman, D. G., Barrow, C. J., Iwashita, T., Kazuo, T., & Patel, D. J. (1991) *Biochemistry* 30, 8009-8017.